

CHIRAL SYMMETRY BREAKING AND COLOR SUPERCONDUCTIVITY IN THE INSTANTON PICTURE

GREGORY W. CARTER

The Niels Bohr Institute, Blegdamsvej 17, 2100 Copenhagen, Denmark

DMITRI DIAKONOV

NORDITA, Blegdamsvej 17, 2100 Copenhagen, Denmark

The instanton approach to spontaneous chiral symmetry breaking is reviewed, with emphasis on the connection to chiral random matrix theory. We extend the approach to discuss the finite density, zero-temperature behaviour of quark matter. Since the instanton-induced interactions are attractive in both $\bar{q}q$ and qq channels, a competition ensues between phases of matter with condensation in either or both. It results in chiral symmetry restoration due to the onset of diquark condensation, a ‘colour superconductor’, at finite density.

1 Why Use Instantons?

The idea that the QCD partition function is dominated by instanton fluctuations of the gluon field, with quantum oscillations about them, has successfully confronted many facts we know about the zero-temperature, zero-density hadronic world (for reviews see refs. ^{1,2}). Instantons have been reliably identified in lattice simulations (for a review see ref. ³). From the theory side, the instanton vacuum constructed from the Feynman variational principle⁴, gives an example of how the necessary ‘transmutation of dimensions’ can actually happen in QCD, meaning that all dimensional quantities can be expressed through the QCD scale parameter, Λ_{QCD} .

2 Instanton Partition Function

The strategy of the instanton approach is to replace the partition function of full QCD with a sum over instantons and quantum fluctuations about them. In particular, the result is an integration over collective coordinates of instantons. A finite-density extension of this model is presumed valid for quark chemical potentials less than approximately 600 MeV, a scale set by the instantons themselves.

The QCD partition function is approximated in two steps. First, the gluon degrees of freedom are replaced with a sum over an ensemble of instantons (I 's) and anti-instantons (\bar{I} 's) with quantum fluctuations above the

non-perturbative vacuum. Explicitly, we write

$$A_\mu = \sum A_\mu^I(\xi) + \sum A_\mu^{\bar{I}}(\xi) + B_\mu, \quad (1)$$

where B_μ are quantum fluctuations above the instanton vacuum and ξ are the collective instanton coordinates comprised of positions, sizes, and colour orientations. With this ansatz, the partition function, including the quark chemical potential, is

$$\mathcal{Z} = \sum \frac{1}{N_+!N_-!} \int d\xi \mathcal{D}B_\mu e^{-U_{inst}(\xi)} \frac{\det(i\nabla + im - i\mu\gamma_4)\det(i\partial + iM)}{\det(i\nabla + iM)\det(i\partial + im)}. \quad (2)$$

Here m is a current quark mass, whereas M is a Pauli-Villars regulator mass. This expression provides a lower bound on the partition function⁴.

Next, the quark determinant is partitioned into high and low momentum contributions. These regimes are divided by an arbitrary mass parameter M_1 , which is chosen large enough such that Det_{high} is factorizable and small enough so that Det_{low} is saturated by the zero modes⁵. With it, we partition as

$$\begin{aligned} \text{Det} &= \text{Det}_{low} \cdot \text{Det}_{high} \\ \text{Det}_{low} &= \frac{\det(i\nabla + im - i\mu\gamma_4)\det(i\partial + iM_1)}{\det(i\nabla + iM_1)\det(i\partial + im)} \\ \text{Det}_{high} &= \frac{\det(i\nabla + iM_1)\det(i\partial + iM)}{\det(i\partial + iM_1)\det(i\nabla + iM)} \end{aligned} \quad (3)$$

If we consider the fields B_μ to be perturbative and subsequently disregard their contributions, we may perform the averaging over the background gauge fields represented by instantons. For the low momentum part one gets the form⁵:

$$\mathcal{Z}_{low} = \sum_{N_\pm} \frac{e^{i\theta(N_+ - N_-)}}{N_+!N_-!} \int \prod_{I\bar{I}} d^4 z_I d\rho_I d\mathcal{O}_I d(\rho_I) \prod_f^{N_f} \begin{pmatrix} im_f & T_{I\bar{I}} \\ T_{\bar{I}I} & im_f \end{pmatrix} \quad (4)$$

The T matrix is of size $N_+ \times N_-$, where N_\pm are the number of I 's and \bar{I} 's, and is comprised of the overlaps of would-be zero modes,

$$T_{I\bar{I}} = \int d^4 x \tilde{\Phi}_0(x - z_I, \rho_I, \mathcal{O}_I; \mu)(i\partial - i\mu\gamma_4)\Phi_0(x - z_{\bar{I}}, \rho_{\bar{I}}, \mathcal{O}_{\bar{I}}; \mu). \quad (5)$$

These integrals are not only functions of the instanton coordinates, but have parametric dependence on chemical potential and temperature as well.

3 Chiral Symmetry Breaking by Instantons

The instanton partition function may be analyzed in three ways, each conceptually quite different but leading to equivalent results. In each case, the main result is spontaneous breaking of chiral symmetry in the vacuum. This phenomena can be interpreted as a delocalization of the “would-be” zero modes, induced by the background instantons, resulting from quarks hopping between them⁵. It was first noticed in ref. ⁶ that there is a far reaching analogy between chiral symmetry breaking in QCD and the problem of electrons in condensed matter systems with random impurities. The acquisition of a dynamical (sometimes called constituent) mass by a quark is fully analogous to the appearance in the Green function of an electron in a metal of a finite relaxation time (but in our case this time depends on the momentum). The appearance of the massless pole in the pseudoscalar channel corresponding to the Goldstone pion is analogous to the formation of a diffusion mode in the density-density correlation function. For the recent development of these and related ideas, see Refs. ⁷ and references therein.

3.1 Random Matrices Approach

Eq. (4) is a particular (and historically first) example of a matrix approach to chiral symmetry breaking. The matrices here are made of the overlaps $T_{I\bar{I}}$ of the would-be fermion zero modes in the background of instantons whose positions, sizes and orientations are random. To make a quick estimate of the spectral density of the Dirac operator, $\nu(\lambda)$, one can use the cluster decomposition in the elements of the $T_{I\bar{I}}$ matrix⁵:

$$\nu(\lambda) = \overline{\sum_n \delta(\lambda - \lambda_n)} = \int \frac{ds}{2\pi} e^{-is\lambda} \overline{\text{Tr} e^{isT}}, \quad (6)$$

where the averaged trace over an ensemble of matrices is expanded as

$$\overline{\text{Tr} e^{isT}} = N \exp \left\{ is \frac{1}{N} \overline{\text{Tr} T} + \frac{(is)^2}{2} \left[\frac{1}{N} \overline{\text{Tr} T^2} - \frac{1}{N^2} \overline{\text{Tr} T}^2 \right] + \dots \right\}. \quad (7)$$

The first term vanishes upon averaging. From the leading cumulant one has

$$\nu(\lambda) = \frac{N}{\sqrt{2\pi\kappa^2}} e^{-\frac{\lambda^2}{2\kappa^2}}, \quad (8)$$

where N is the total number of I 's and \bar{I} 's and the parameter κ is the average overlap of zero modes:

$$\kappa^2 = \frac{1}{N} \overline{\text{Tr} [T_{I\bar{I}} T_{\bar{I}I}]} = \text{const} \cdot \frac{N}{V} \bar{\rho}^2, \quad (9)$$

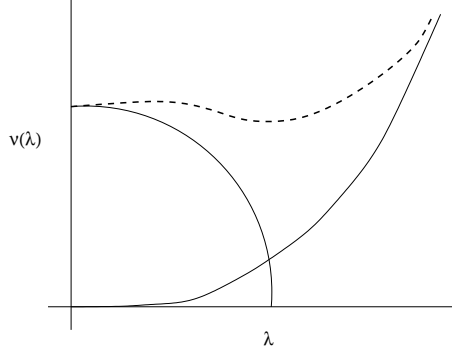


Figure 1. Schematic eigenvalue distribution of the Dirac operator. The solid lines are the zero mode and free contributions, the dashed line an estimate of the full spectrum.

with $\bar{\rho}^2$ being the average size of instantons obtained from the size distribution $d(\rho_I)$ of eq. (4).

Using the first cumulant in eq. (7) is, however, incomplete. Resumming all contributions yields the Wigner semicircle spectrum:

$$\nu(\lambda) = \frac{N}{\pi\kappa} \sqrt{1 - \frac{\lambda^2}{4\kappa^2}}. \quad (10)$$

The chiral condensate is obtained directly from this result via the Banks-Casher relation. With the average instanton density N/V and sizes $\bar{\rho}$ commonly used for the instanton medium, one gets the reasonable

$$\langle \bar{\psi}\psi \rangle_0 = -\frac{\pi\nu(0)}{V} = -\frac{2N}{\kappa V} \sim \frac{1}{R^2\bar{\rho}} \approx -(255 \text{ MeV})^3. \quad (11)$$

We note that the spectrum-smearing parameter κ is a small number – approximately 100 MeV. One likewise obtains a good approximation to the pion decay constant, finding $f_\pi \simeq 100$ MeV, comparable to its well-known experimental value of 93 MeV^{5,6}.

There is naturally more to the spectrum than the zero modes; minimally, the high-momentum modes which can be approximated by those of free quarks. The eigenvalue density obtained from this part of the spectrum is

$$\nu(\lambda) \approx \frac{N_c}{4\pi^2} \lambda^3. \quad (12)$$

The full spectrum, shown schematically in Fig. 1, is a combination of this, the Wigner semicircle, and the intermediate modes which are ignored in this treatment.

It was noticed by Simonov⁸ that the partition function (4) can be generalized to the schematic form of a random matrix integrated with some weight whose precise form is not essential because of the ‘universality’. This allows an economical rewriting:

$$\mathcal{Z}_{low} = \int dT P(TT^\dagger) \det \begin{bmatrix} im & T \\ T^\dagger & im \end{bmatrix}. \quad (13)$$

With an exponential weight, the form of eq.(13) is the partition function of chiral random matrix theory, from which one obtains the Wigner semicircle⁸, see also Ref. ⁹. Later on, eq.(13) became a base of a now well-developed study of the microscopic spectral density of the Dirac operator and their correlations; see J. Verbaarschot, these proceedings.

At finite density, the expressions must naturally be modified. This has been done in a schematic way with random matrices¹⁰. In the instanton picture, we retain the microscopic physics of the zero mode solution at finite chemical potential, which shall be discussed in what follows.

3.2 Propagator Approach

The random matrices approach is, unfortunately, limited to the spectral density: it cannot be used to study the x -dependent correlation functions related to chiral symmetry breaking. Knowing the microscopic origin of the random matrices $T_{I\bar{I}}$ as due to the overlap of the instanton zero modes, allows one to calculate those quantities.

The simplest quantity is the ensemble-averaged quark propagator computed in refs. ⁵ (second and third reference) and in ref. ¹¹. The propagating quark interacts with the background via the would-be zero modes, quantified in the same overlap matrices T_{IJ} used previously. It has the averaged form:

$$S(x-y) = \overline{\Phi_I^*(x-z_I) \frac{1}{im + T_{IJ}} \Phi_J(y-z_J)} = \frac{1}{\not{p} - iM(p)}. \quad (14)$$

The result is a dynamical quark mass $M(p) = const \cdot \sqrt{\bar{\rho}^2 N/V} F(p\bar{\rho})$, where $F(p\bar{\rho})$ is a function known analytically and features a natural cutoff at momentum $p\bar{\rho} = 1$.

Closing a quark loop with this effective propagator generates a ‘gap equa-

tion' encoding the instanton density dependence of the dynamical mass⁵,

$$\frac{N}{V} = 4N_c \int \frac{d^4p}{(2\pi)^4} \frac{M(p)^2}{p^2 + M(p)^2}. \quad (15)$$

Since it has a solution with $M(p) \neq 0$, even for a zero current quark mass m , it implies spontaneous chiral symmetry breaking. A nonzero current quark mass m can be also incorporated in this approach^{5,11}. Knowing the propagator $S(x, y; m)$ one can find the determinant for low-momentum modes according to a general formula

$$\begin{aligned} \text{Det}_{low} &= \exp \int_m^{M_1} dm' [S(x, x; m') - S_0(x, x; m')] \\ &= \exp \left\{ -N \int_m^{M_1} dm' \frac{1}{2\kappa^2} \left(\sqrt{m'^2 + 4\kappa^2} - m' \right) \right\}. \end{aligned} \quad (16)$$

Comparing it with another representation,

$$\text{Det}_{low} = \exp \left(\frac{1}{2} \int d\lambda \nu(\lambda) \ln \frac{\lambda^2 + m^2}{\lambda^2 + M_1^2} \right), \quad (17)$$

one recovers the semicircle spectrum, eq.(10). It demonstrates the mathematical equivalence of the propagator and the random matrices approaches, though the first method is more powerful as it allows one to compute also x -dependent correlations^{5,6}. In both cases the large- N_c approximation has been exploited.

3.3 Effective Lagrangian Approach

In the previous section the effective quark propagator was obtained by averaging the instanton background's effects on a single quark. One can recover identical physics by first averaging over instantons at the level of the partition function. The result is an effective action for quarks which contains instanton effects in induced multi-quark interactions. The would-be zero modes serve here as a bridge, passing information from the instanton vacuum to the effective quarks through the induced vertex. The consequent interactions are vertices involving $2N_f$ quarks, commonly cited as 't Hooft interactions since he was the first to specify the proper quantum numbers.

The overall strength of this interaction is not fixed once and forever but rather has to be integrated over all possible values, since it technically appears as a Lagrange multiplier¹. Fortunately, in the thermodynamic limit one finds the integral is completely determined by its saddle-point result. Denoting the

coupling constants λ_{\pm} , the result for the low-momentum partition function is^{1,12}

$$\mathcal{Z} = \int d\lambda_+ d\lambda_- \int D\psi D\psi^\dagger \exp \left\{ \int d^4x \psi^\dagger (i\cancel{\partial} - i\mu\gamma_4)\psi + \lambda_+ Y_{N_f}^+ + \lambda_- Y_{N_f}^- \right. \\ \left. + N_+ \left(\ln \frac{N_+}{\lambda_+ V} - 1 \right) + N_- \left(\ln \frac{N_-}{\lambda_- V} - 1 \right) \right\}. \quad (18)$$

The left-handed vertex,

$$Y^+[\psi, \psi^\dagger] = \int dU \int \prod_f^{N_f} \left[\frac{(d^4 p_f d^4 k_f)}{(2\pi)^8} \right] (2\pi)^4 \delta^4 \left(\sum (p_f - k_f) \right) \prod_f^{N_f} \left[U_{l_f}^{\alpha_f} U_{\beta_f}^{\dagger o_f} \right. \\ \left. \cdot \psi_{L f \alpha_f i_f}^\dagger(p_f) \mathcal{F}(p_f, \mu)_{k_f}^{i_f} \epsilon^{k_f l_f} \epsilon_{n_f o_f} \mathcal{F}^\dagger(k_f, -\mu)_{p_f}^{n_f} \psi_L^{f \beta_f p_f}(k_f) \right] \quad (19)$$

contains the matrix form factors

$$\mathcal{F}(p, \mu) = (p + i\mu)^- \varphi(p, \mu)^+, \quad \mathcal{F}^\dagger(p, -\mu) = \varphi^*(p, -\mu)^- (p + i\mu)^+. \quad (20)$$

The $\varphi(p, \mu)$ are the Fourier-transformed zero mode solutions and we use the notation $x^\pm = x^\mu \sigma_\mu^\pm$, where the 2×2 matrices $\sigma_\mu^\pm = (\pm i\vec{\sigma}, 1)$ decompose the Dirac matrices into chiral components, and it is understood that μ written as a four-vector is $\mu_\alpha = (\vec{0}, \mu)$. A similarly defined Y^- carries right-handed quarks. All calculations discussed here are in the topologically neutral case, where $N_+ = N_- = N$ and hence $\lambda = \lambda_+ = \lambda_-$.

With a Fierz decomposition, the instanton-induced interaction can easily be made to resemble the Nambu–Jona-Lasinio model. However, in the steps leading to this result, microscopic information has been retained. Instantons not only provide a natural cutoff through the form factors and a dynamically determined coupling strength, but also account for anomalously broken $U_A(1)$ symmetry and correctly reproduce $SU(4)$ Pauli–Gürsey symmetry when $N_c = 2$. It should be also added that the naive addition of a nonzero current quark mass to the NJL Lagrangian fails to reproduce several known low-energy Ward identities, as well as the phenomenologically-known coefficients in the Gasser–Leutwyler chiral Lagrangian (the terms containing m^2 and $m \cdot p^2$). The microscopic instanton approach preserving all symmetries of QCD is capable to correctly incorporate nonzero quark masses, and it does so in a rather nontrivial way¹³.

4 Competition Between $\bar{q}q$ and qq Channels

Since the instanton-induced interactions (19) support both $\bar{q}q$ and qq condensation, it is necessary to consider the two competing channels simultaneously. This means that one must calculate both the normal (S) and anomalous (F) quark Green functions. A colour/flavour/spin ansatz compatible with the possibility of chiral and colour symmetry breaking is

$$\begin{aligned}\langle \psi^{f\alpha i}(p)\psi_{g\beta j}^\dagger(p) \rangle &= \delta_g^f \delta_\beta^\alpha S_1(p)_j^i \quad \text{for } \alpha, \beta = 1, 2, \\ \langle \psi^{f\alpha i}(p)\psi_{g\beta j}^\dagger(p) \rangle &= \delta_g^f \delta_\beta^\alpha S_2(p)_j^i \quad \text{for } \alpha, \beta > 2, \\ \langle \psi_L^{f\alpha i}(p)\psi_L^{g\beta j}(-p) \rangle &= \langle \psi_R^{f\alpha i}(p)\psi_R^{g\beta j}(-p) \rangle = \epsilon^{fg} \epsilon^{\alpha\beta[\gamma]} \epsilon^{ij} F(p),\end{aligned}\quad (21)$$

where $[\gamma]$ refers to some generalized direction(s) in colour space, and it is this set of $N_c - 2$ indices which signals the breaking of colour symmetry. In the particular case of $N_c = 3$, where the colour symmetry is broken as $SU(3) \rightarrow SU(2) \times U(1)$ and our ansatz considers the $\bar{3}$ channel, we will by convention take $[\gamma] = 3$; for $N_c = 4$ one can take $[\gamma] = 34$ and so forth. In the event of colour symmetry breaking, the standard propagators (and ensuing condensates) will lose their colour degeneracy and the separation of $S(p)$ into $S_1(p)$ and $S_2(p)$ becomes necessary; otherwise the Schwinger-Dyson-Gorkov equations do not close¹².

Written in the chiral L, R basis, the 4×4 propagators $S_{1,2}(p)$ are of the form:

$$S(p) = \begin{bmatrix} G(p)\mathbf{1} & Z(p)\mathbf{S}_0(p)^+ \\ Z(p)\mathbf{S}_0(p)^- & G(p)\mathbf{1} \end{bmatrix}. \quad (22)$$

Here the off-diagonal, bare propagator $\mathbf{S}_0(p)^\pm = [(p + i\mu)^\mp]^{-1}$ is modified by the scalar functions $Z_{1,2}(p)$, and is augmented on the diagonal by the scalar $G_{1,2}(p)$ which if nonzero break chiral symmetry.

Using the instanton-induced interaction (19) directly, without Fierz rearrangement, one can build a systematic expansion for the F, G Green functions in the parameters $1/N_c$ and $\bar{\rho}/\bar{R}$. In the leading order in both parameters we restrict ourselves to the one-loop approximation shown in Fig. 2. It corresponds to a set of self-consistent Schwinger-Dyson-Gorkov equations. An important μ -dependence enters through the form factors in eq. (19).

4.1 The System of Gap Equations

This system of equations reduces to a set of three gap equations which self-consistently specify three condensates: two chiral and one diquark. They are

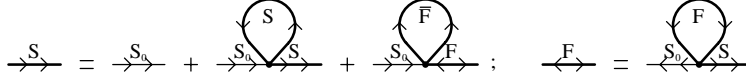


Figure 2. Schwinger-Dyson-Gorkov diagrams to first order in λ .

defined as the closed loops:

$$g_{1,2} = \frac{\lambda}{N_c^2 - 1} \int \frac{d^4 k}{(2\pi)^4} A(k, \mu) G_{1,2}(k); \quad f = \frac{\lambda}{N_c^2 - 1} \int \frac{d^4 k}{(2\pi)^4} B(k, \mu) F(k). \quad (23)$$

The functions $A(k, \mu)$ and $B(k, \mu)$ are scalar functions which arise from spin-averaging the matrix form factors, as defined in ref. ¹². The quantities $M_{1,2}$ and Δ are linear combinations of the condensates $g_{1,2}$ and f :

$$\begin{aligned} M_1 &= (5 - 4/N_c) g_1 + (2N_c - 5 + 2/N_c) g_2, \\ M_2 &= 2(2 - 1/N_c) g_1 + 2(N_c - 2) g_2, \quad \Delta = (1 + 1/N_c) f. \end{aligned} \quad (24)$$

The $M_{1,2}$ are measures of chiral symmetry breaking, which act as an effective mass modifying the standard quark propagation. On the other hand the diquark loop 2Δ plays the role of twice the single-quark energy gap formed around the Fermi surface.

The solution of the gap equations depends on the vertex coupling constant, λ , which itself is determined by balancing the instanton background with the condensates through its saddle-point value. This minimization of the partition function (18) leads to

$$\frac{N}{V} = \lambda(Y^+ + Y^-) = \frac{4(N_c^2 - 1)}{\lambda} [2g_1 M_1 + (N_c - 2)g_2 M_2 + 4f\Delta]. \quad (25)$$

This joins the gap equations to close a system of equations, numerically solvable.

Once this is done, the chiral condensate proper may be computed as an integral over the resummed propagator:

$$-\langle \bar{\psi}\psi \rangle_{Mink} = i\langle \psi^\dagger\psi \rangle_{Eucl} = 4 \int \frac{d^4 p}{(2\pi)^4} [2G_1(p) + (N_c - 2)G_2(p)]. \quad (26)$$

4.2 Thermodynamic Competition

For any given chemical potential, multiple solutions can be obtained for the gaps. These correspond to different phases of quark matter, and they are summarized as follows:

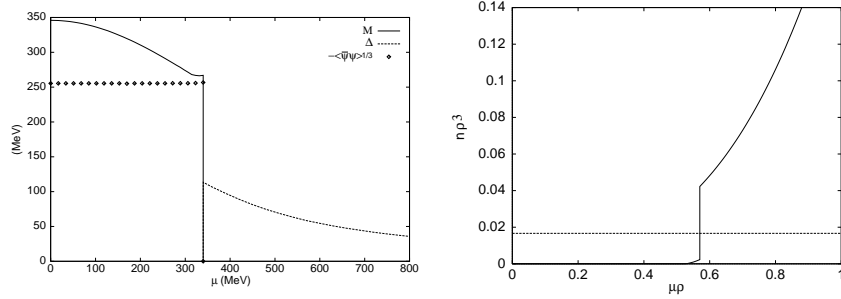


Figure 3. Left panel: Condensates for $N_c = 3$ as a function of μ . Shown are the effective quark mass M , the quark condensate $-\langle\bar{\psi}\psi\rangle^{1/3}$, and the diquark energy gap per quark Δ . Right Panel: The quark density n_q vs. μ .

- (0) Free massless quarks: $g_1 = g_2 = f = 0$.
- (1) Pure chiral symmetry breaking: $g_1 = g_2 \neq 0, f = 0$.
- (2) Pure diquark condensation: $g_1 = g_2 = 0, f \neq 0$.
- (3) Mixed symmetry breaking: $g_1 \neq g_2 \neq 0, f \neq 0$.

The free energy, calculated to first order in λ , is minimized in order to resolve the stable solution. The phase corresponding to the *lowest* coupling λ is the thermodynamically favoured¹².

No solutions were found matching Phase (0), and the Phase (3) solution obtained disappears at relatively low chemical potential ($\mu \approx 80$ MeV) and is never thermodynamically competitive¹². The remaining phase competition is then between Phases (1) and (2). In the vacuum, where $\mu = 0$, one finds Phase (1) preferred – this is the standard picture. However, at a critical chemical potential μ_c , defined by the ratio of superconductive gap to chiral effective masses

$$\frac{\Delta(\mu_c)}{M(\mu_c)} = \sqrt{\frac{N_c}{8(N_c - 1)}} = \frac{\sqrt{3}}{4}, \quad (27)$$

a first-order phase transition occurs. With the standard instanton parameters $N/V = 1 \text{ fm}^{-4}$ and $\bar{\rho} = 0.33 \text{ fm}$, we find $\mu_c \simeq 340$ MeV. This and the first-order nature of the phase transition are clearly seen in Fig. 3.

The quark density is physically more relevant than the chemical potential. Thus we calculate

$$n_q = \int d^4x j_4(x) = -i \int \frac{d^3p}{(2\pi)^3} n(p), \quad (28)$$

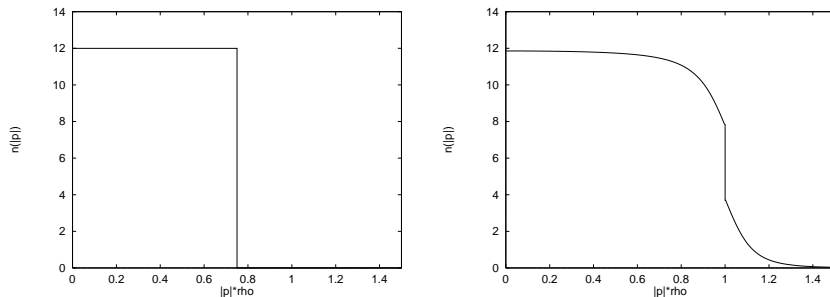


Figure 4. Occupation number $n(p)$ vs. p for Phase (1) (left panel) and Phase (2) (right panel) for $\mu = 1/\bar{\rho} = 600$ MeV.

where we have defined the occupation number density for quarks as $n(|\vec{p}|)$ as an intermediate step. The correct, conserved form of the quark current is given in ref. ¹². Here we present only numerical results, in Figs. 3 and 4. In Phase (1), there is clearly an effective mass brought about by spontaneous symmetry breaking, indicated by the reduced Fermi radius. We stress that, despite the complicated four-momentum dependence of the interaction, the resulting occupation number density appears as a perfect Fermi step function. Cooper pairing, however, smears the Fermi surface, and this is evinced in the second plot. The residual discontinuity at $|\vec{p}| = \mu$ is the contribution from the free, colour-3 quarks which do not participate in the diquark. Those that do are smoothly distributed as a Bosonic condensate.

Performing the integration over three-momenta, we arrive at the density as a function of chemical potential. In the right panel of Fig. 3 this is shown for the equilibria states, demonstrating the large discontinuity at the phase transition, where the horizontal line signifies the quark density of equilibrium nuclear matter. The phase transition occurs at an extremely low quark density, a conceptual conundrum which is seeing ongoing discussion in the literature^{12,14,15,16,17}.

5 Conclusions

We have discussed three ways of obtaining the spontaneous breaking of chiral symmetry in the instanton approach. While the physics of each seem superficially distinct, it has been demonstrated that they are equivalent. One of these approaches was extended for and applied to finite density quark matter, where a chiral symmetry restoring, first order phase transition reorders

the quarks into a colour superconducting medium. These results agree with related works, but unfortunately also share a mysteriously low transition density, a mere fraction of that corresponding to equilibrium nuclear matter.

References

1. D. Diakonov, in: *Selected Topics in Non-perturbative QCD*, Proc. Enrico Fermi School, Course CXXX, A.Di Giacomo and D.Diakonov, eds., Bologna, (1996) p.397, hep-ph/9602375
2. T. Schäfer and E. Shuryak, *Rev. Mod. Phys.* **70**, 323 (1998).
3. P. van Baal, *Nucl. Phys. B*(Proc. Suppl.) **63**, 126 (1998).
4. D. Diakonov and V. Petrov, *Nucl. Phys. B* **245**, 259 (1984); D. Diakonov, M. Polyakov and C. Weiss, *Nucl. Phys. B* **461**, 539 (1996).
5. D. Diakonov and V. Petrov, *Phys. Lett. B* **147**, 351 (1984); *Sov. Phys. JETP* **62**, 204 (1985); *Nucl. Phys. B* **272**, 457 (1986).
6. D. Diakonov and V. Petrov, *Sov. Phys. JETP* **62**, 431 (1985).
7. R.A. Janik, M.A. Nowak, G. Papp, and I. Zahed, *Phys. Rev. Lett.* **81**, 264 (1998); J.C. Osborn, D. Toublan and J.J. Verbaarschot, *Nucl. Phys. B* **540**, 317 (1999);
8. Yu.A. Simonov, *Phys. Rev. D* **43**, 3534 (1991).
9. M.A. Nowak, J.J. Verbaarschot, and I. Zahed, *Phys. Lett. B* **217**, 157 (1989).
10. A.M. Halasz, A.D. Jackson, and J.J.M. Verbaarschot, *Phys. Rev. D* **56**, 5140 (1997); R.A. Janik, M.A. Nowak, G. Papp, and I. Zahed, *Phys. Rev. Lett.* **77**, 4876 (1996).
11. P. Poblitsa, *Phys. Lett. B* **226**, 387 (1989).
12. G.W. Carter and D. Diakonov, *Nucl. Phys. A* **642**, 78c (1998); *Phys. Rev. D* **60**, 016004 (1999).
13. M. Musakhanov, hep-ph/9810295.
14. M. Alford, K. Rajagopal, and F. Wilczek, *Phys. Lett. B* **422**, 247 (1998); R. Rapp, T. Schäfer, E.V. Shuryak and M. Velkovsky, *Phys. Rev. Lett.* **81**, 53 (1998).
15. J. Berges and K. Rajagopal, *Nucl. Phys. B* **538**, 215 (1999).
16. M. Buballa, *Nucl. Phys. A* **611**, 393 (1996).
17. J. Berges, D.-U. Jungnickel, and C. Wetterich, *Quark and Nuclear Matter in the Linear Chiral Meson Model*, hep-ph/9811387.

